Original Paper

European Surgical Research

Eur Surg Res 2011;47:222–230
DOI: 10.1159/000333088

Received: April 12, 2011
Accepted after revision: July 20, 2011
Published online: November 2, 2011

Morphology and Hemodynamics during Vascular Regeneration in Critically Ischemic Murine Skin Studied by Intravital Microscopy Techniques

R. Schweizer[a] K. Merz[d] S. Schlosser[a] T. Spanholtz[a] C. Contaldo[e] J.V. Stein[c]
V. Enzmann[a, b] P. Giovanoli[e] D. Erni[d] J.A. Plock[a, d, e]

Departments of [a]Clinical Research and [b]Ophthalmology, and [c]Theodor Kocher Institute, University of Bern, [d]Department of Plastic and Hand Surgery, Inselspital, University Hospital, Bern, and [e]Division of Plastic and Hand Surgery, University Hospital, Zürich, Switzerland

Key Words
Angiogenesis · Arteriogenesis · Hypoxia · Intravital microscopy · Microcirculation · Surgical flap · Neovascularization · Vascular remodeling

Abstract
Background: With the understanding of angiogenesis and arteriogenesis, new theories about the orchestration of these processes have emerged. The aim of this study was to develop an in vivo model that enables visualization of vascular regenerating mechanisms by intravital microscopy techniques in collateral arteriolar flap vascularity. ***Methods:*** A dorsal skin flap (15 × 30 mm) was created in mice and fixed into a skinfold chamber to allow for assessment of morphology and microhemodynamics by intravital fluorescence microscopy (IVFM). Laser scanning confocal microscopy (LSCM) was utilized for three-dimensional reconstruction of the microvascular architecture. ***Results:*** Flap tpO_2 was 5.3 ± 0.9 versus 30.5 ± 1.2 mm Hg in controls ($p < 0.01$). The collateral arterioles in the flap tissue were dilated (29.4 ± 5.3 μm; $p < 0.01$ vs. controls) and lengthened in a tortuous manner (tortuosity index 1.00 on day 1 vs. 1.35± 0.05 on day 12; $p < 0.01$). Functional capillary density was increased from 121.00 ± 25 to 170 ± 30 cm/cm^2 (day 12; $p < 0.01$) as a result of angiogenesis. Morphological evidence of angiogenesis on capillary level and vascular remodeling on arteriolar level could be demonstrated by IVFM and LSCM. ***Conclusions:*** Present intravital microscopy techniques offer unique opportunities to study structural changes and hemodynamic effects of vascular regeneration in this extended axial pattern flap model.

Copyright © 2011 S. Karger AG, Basel

Introduction

Critical ischemia and hypoxia can lead to consecutive functional loss, cell death and necrosis in surgical flaps. During the last years, a new approach to tackle critical ischemia has emerged, which consists in promoting the regenerative potential of the vasculature to compensate the diminished supply of blood and oxygen. Such neovascularization includes the formation of new vessels (angiogenesis) and the remodeling (arteriogenesis) of preexisting vascular structures. Up to date, each of these mechanisms has predominantly been investigated as an isolated process, whereas there is a paucity of data documenting these integral processes in the living tissue over time. Previous in vivo studies have been restricted to the analysis of necrotic flap area or single time-point experiments, or focused on acute phenomena of vasoregulation [1, 2], ischemia and ischemia reperfusion experiments [3–

KARGER

Fax +41 61 306 12 34
E-Mail karger@karger.ch
www.karger.com

© 2011 S. Karger AG, Basel
0014–312X/11/0474–0222$38.00/0

Accessible online at:
www.karger.com/esr

Jan A. Plock, MD
Department of Clinical Research, University of Bern
Murtenstrasse 50
CH–3010 Bern (Switzerland)
E-Mail jan.plock@dkf.unibe.ch

source: https://doi.org/10.48350/4540 | downloaded: 11.5.2024

Downloaded from http://karger.com/esr/article-pdf/47/4/222/2738393/000333088.pdf by UniversitÄtsbibliothek Bern user on 21 June 2023

5] and tissue survival studies [6, 7]. Recently, the attempt has been made to study angiogenesis over time [6, 8]. The physiological vascular regeneration mechanisms following critical ischemia without development of necrosis are, however, fairly evaluated continuously and morphologically over time, which is especially true for extended axial pattern flaps with collateralized random perfusion in the extended part.

Various techniques have been used to demonstrate oxygen delivery [9], oxygen homeostasis or blood flow by dye diffusion [10], laser Doppler flowmetry [11], oxygen measurements [12, 13] or microdialysis [14–16]. However, all these techniques have their limitations in assessing blood perfusion only indirectly.

The missing link between basic knowledge and biological efficacy of neovascularization may be substituted using intravital microscopic techniques repetitively providing in vivo data of both the regenerative morphological changes and their hemodynamic effects simultaneously [2, 17–19]. Intravital fluorescence microscopy (IVFM) is the only technique that allows for direct and quantitative assessment of hemodynamic and morphological data in the living tissue over time. With the aid of a variety of dyes, high-resolution optical instrumentation and sophisticated software, all levels of the vascular network can be investigated [6, 8]. In addition, oxygenation and viability can be monitored in the same tissue. The shortcoming of IVFM, e.g. two-dimensional imaging and limited penetration depth, can be circumvented by utilizing multiphoton laser scanning confocal microscopy (LSCM) [20, 21], which has been shown to enable three-dimensional reconstruction of living tissue structures with a resolution that allows for visualization of cellular organelles at a penetration depth of several hundred micrometers [22].

The present study was dedicated to the development of a new application of the dorsal skinfold chamber that enables studying vascular regenerative mechanisms with intravital microscopy techniques in order to follow the interrelationship between the morphological vascular changes resulting from neovascularization and microhemodynamic changes on various vascular levels over time. The focus was put on the arteriolar collateralization zone of an extended axial pattern flap.

Animals and Methods

The experiments were performed according to the National Institutes of Health guidelines for the care and use of laboratory animals and with the approval of the local Animal Ethics Committee.

Animals

Twenty-six female mice (C57BL/6, 10–12 weeks old, 23–25 g; Charles River Laboratories, Sulzfeld, Germany) were used in this study. The animals were housed in single cages postoperatively with free access to water and standard diet. Due to the lack of optical clarity, anesthesia complications and infection, 6 animals were excluded in the early phase of the experiments. Ten animals were available for analysis in the flap and skin chamber group, 6 animals were included in the control group after receiving a skin chamber only. These groups were also used for tpO_2 and microdialysis measurements on day 1. Another 4 animals were assigned to analysis by LSCM after flap and skin chamber operation.

Anesthesia

For all manipulations, the animals were anesthetized with an intraperitoneal injection of medetomidine 500 μg/kg body weight (BW), climazolam 5 mg/kg BW, and fentanyl 50 μg/kg BW. Reversion was induced by antidote injection with atipamezol 1.25 mg/kg BW (Antisedan; Pfizer, Switzerland), sarmazenil 0.5 mg/kg BW (Sarmasol; Gräub, Switzerland) and naloxon 0.6 mg/kg BW (Naloxon; Orpha, Switzerland) after the manipulations were completed.

Flap Surgery

The anesthetized animals were placed on a heating pad in a prone position, and the room temperature was set at 28°C to keep their skin temperature constant at 32°C, which was verified with a microthermometer placed on the abdominal skin. The back skin was shaved and depilated. Surgery was performed with the aid of an operating microscope at ×10 magnification (Wild Heerbrugg, Switzerland). The flap was planned as a cranially pedicled axial pattern flap, nourished by the lateral thoracic artery, with a length-to-width ratio of 30 × 15 mm. The spine was taken as medial flap border. The flap consisted of skin, a thin layer of panniculus carnosus muscle, and subcutaneous tissue. During surgery, the flap was irrigated with 0.9% NaCl to prevent it from drying out. The flap was fixed into a dorsal skin fold chamber to make it amenable to intravital microscopy (fig. 1).

Wound infection and technical complications such as rupture of the sutures or insufficient optical clarity due to granulation tissue were defined as exclusion criteria.

Three distinct vascular zones were defined within the flap: the proximal zone, corresponding to the vascular territory of the flap pedicle, i.e. the lateral thoracic artery; the distal zone corresponding to the territory of the circumflex iliac artery, and the intermediate zone consisting of collateral vessels, through which the distal zone is perfused. In the control group, the skin fold chamber was mounted onto intact skin in the same area. Postoperatively, all animals received analgesic treatment with metamizole (0.25 mg/g BW, Novalgin; Sanofi-Aventis, Switzerland) and 0.1 ml glucose 5% for volume replacement purposes due to the large wound size.

Tissue Oxygenation

To measure tissue oxygenation, a 22-gauge needle was inserted in the tissue. After removing the canula, the measuring probes could be inserted in the preformed duct. Care was taken not to injure larger vessels, which would lead to bleeding and prohibit adequate measurement.

Downloaded from http://karger.com/esr/article-pdf/47/4/222/2738393/000333088.pdf by UniversitÄtsbibliothek Bern user on 21 June 2023

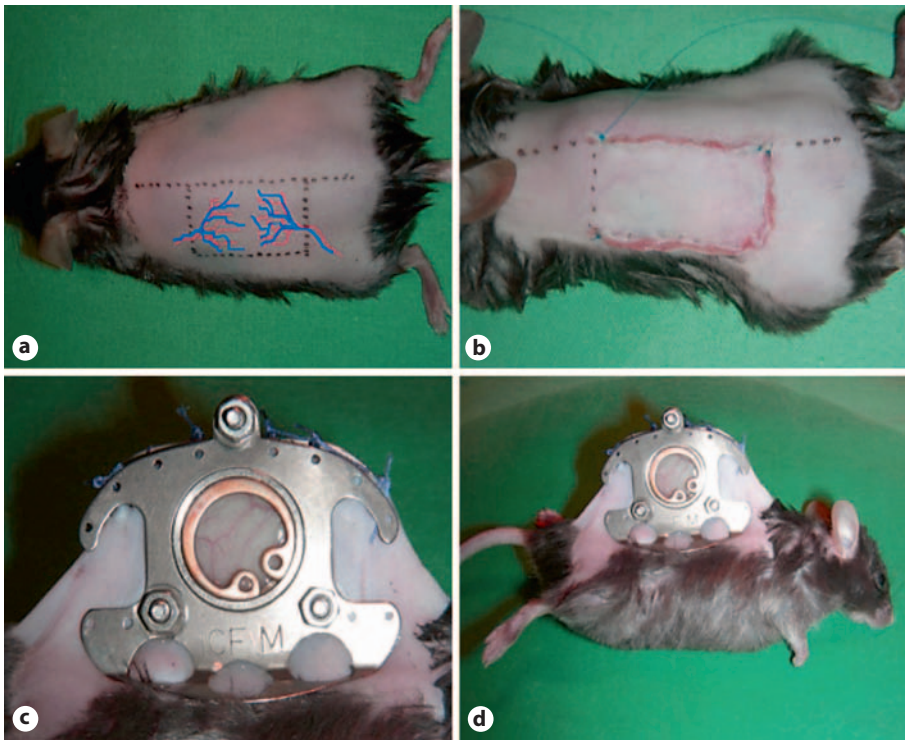

Color version available online

Fig. 1. Surgical flap model with the marked area including the two vascular territories of the lateral thoracic and the superficial circumflex iliac artery (**a**), which is secured during surgery (**b**). The flap is mounted into a dorsal skin chamber (**c**) and available for intravital microscopy examinations (**d**).

Partial oxygen tension was assessed in the tissue with Clark-type microprobes consisting of polarographic electrodes and an oxygen-sensitive microcell with a pO_2-sensitive area of 1 mm^2 (Revoxode CC1; GMS, Kiel, Germany) [23, 24]. The probes were inserted into the subcutaneous tissue in the distal vascular territory of the flap under visual control and microscopic magnification. In control animals, the probe was placed in the subcutaneous tissue of the distal part of the chamber window. Care was taken to place the probes away from arterioles and large venules. Equilibration was awaited and values were measured over 5 min.

The microdialyis technique (CMA, Stockholm, Sweden) was utilized for analysis of the oxidative energy metabolism in the jeopardized tissue. Interstitial concentrations of pyruvate and lactate were determined as previously described [12, 24–26]. The lactate-to-pyruvate ratio was calculated to assess the aerobic/anaerobic correlation. Microprobes (CMA20, 20 kDa, PAES; CMA) were perfused with isotonic Ringer solution using a microinjection pump (CMA/100; CMA). The perfusion rate was set to 0.75 μl/min. After insertion in the tissue, probes were perfused for 30 min for equilibration before the definitive sample was collected over 15 min. The dialysates were analyzed photometrically using the CMA600 computer-based system (CMA) [25, 27].

Intravital Fluorescence Microscopy

Investigations were performed using an epiluminescence intravital microscope (Zeiss AxioplanI; Zeiss, Jena, Germany), as reported earlier [2, 12, 23, 28]. Microscopic images were captured by a television camera (intensified CCD camera; Kappa Messtechnik, Gleichen, Germany), displayed on a television screen (Trinitron PVM-1454; Sony, Tokyo, Japan), and recorded on video (50 Hz; Panasonic AG-7350-SVHS, Tokyo, Japan) for subsequent offline analysis with the help of a computer-assisted image analysis system (CapImage; Zeintl, Heidelberg, Germany) [29, 30]. The preparation was observed visually with a ×40 water immersion objective with a numerical aperture of 0.75, which resulted in a total optical magnification of ×909 on the video monitor, where 1 pixel corresponded to 264 nm in the tissue. The microvessels were classified according to physiological and anatomical features. The pedicle artery, collateral arterioles in the proximal part of the flap, capillaries in the distal part of the flap, and postcapillary collecting venules in the distal part of the flap were chosen for evaluation according to their optical clarity. The intraluminal microvascular diameters were measured in micrometers with the use of 2% fluorescein isothiocyanate-labeled-dextran (FITC dextran, 150 kDa; Sigma, Buchs, Switzerland). The tortuosity index was defined as a function of changing vessels, linearity over a defined distance. Briefly, it is determined by the ratio between the length of the winded arteriole and the distance of the starting point and the end point of a determined vessel section. Functional capillary density (FCD) was defined as the length of red blood cell-perfused capillaries per observation area (cm/cm^2). Capillary perfusion was determined by red blood cell velocity (RBC velocity; mm/s) in the capillary system. All measurements were performed using CapImage software (Zeintl).

Leukocytes were stained using rhodamin 6G. As reported earlier [2], leukocyte interaction with the endothelium was analyzed quantitatively. Sticking leukocytes were defined as the number of cells per square micrometer of venular endothelial cell surface (calculated from diameter and length of the vessel segment studied, assuming cylindrical geometry) that remained stationary and

Downloaded from http://karger.com/esr/article-pdf/47/4/222/2738393/000333088.pdf by UniversitÄtsbibliothek Bern user on 21 June 2023

attached for at least 20 s to the microvascular endothelium. Rolling leukocytes were defined as cells moving along the vascular wall more slowly than the blood stream, or leukocytes sticking to the endothelium for less than 20 s. They were reported as the number of cells passing a reference point within the microvessel.

Multiphoton Confocal Microscopy (LSCM)

Multiphoton imaging allowed three-dimensional time-lapse imaging of fluorescent signals deep below the surface of living tissues. The fluorescent images were of slightly lower resolution compared with those obtained by traditional confocal microscopy. Differentiation of differently stained objects was obtained with double- or triple-labeled excitation using a Ti:Al2O3 laser at 800 nm and a HeNe laser at 633 nm. Multiphoton imaging was performed with a fluorescence microscope (BX50WI; Olympus, Volketswil, Switzerland) equipped with a 20× objective and a software-controlled confocal/multiphoton microscopy system (LaVision Biotec, Bielefeld, Germany). For multiphoton excitation and second harmonic generation, a Ti:sapphire laser with a 12-W pump laser (MaiTai HP; Spectra-Physics, Darmstadt, Germany) was tuned to 780 nm. For three-dimensional analysis of vascularity, scans from 500 × 500 × 200 to 50 × 50 × 10 μm (scan field × depth, z-step size of 2 μm) between 10 and 30 μm below the skin were taken using 780 nm excitation wavelength. Fluorescent and second harmonic generation signals were collected using 455/57- and 525/50-nm bandpass filters and 593/40-nm bandpass filters with non-descanned detectors to generate three-color images. Plasma was labeled with FITC dextran (250 kDa, 25 mg/ml; Sigma Chemical, St. Louis, Mo., USA) according to the manufacturer's instructions. Three-dimensional analysis of vascular structures was performed using imaging software (Volocity; Improvision, Lexington, Ky., USA).

Immunohistochemistry

Tissue hypoxia was assessed by pimonidazole staining as established previously [12, 24]. Thirty minutes prior to euthanasia the HypoxyProbe™-1 antibody (60 mg/kg) was administered. Skin samples were taken at the end of the experiment on day 12. Tissue was fixed in 4% paraformaldehyde, washed in PBS, stored in 70% ethanol and finally embedded in paraffin blocks. Five-micron sections were cut, transferred to micro-slides and air-dried at 37°C overnight.

Paraffin sections were dewaxed and rehydrated. For detection of HypoxyProbe, sections were blocked for endogenous peroxidases with 3% H_2O_2 for 5 min followed by 0.01% Pronase for 40 min at 40°C for antigen retrieval. Sections were treated with DAKO blocking solution for 5 min and incubated with HypoxyProbe-1 antibody 1:50 for 40 min, followed by biotin-conjugated $F(ab')_2$ 1:500 and streptavidin peroxidase. Signals were developed using a DAB-peroxidase system (DAKO).

For VEGF staining, the sections were deparaffinized and rehydrated. They were immersed in 0.1 M tri-Na citrate at pH 6.0 and underwent heat-induced antigen retrieval with a microwave oven. After cooling down to room temperature, the slides were rinsed with PBS (2 × 3 min). The sections were incubated with a monoclonal mouse reactive VEGF-antibody (Abcam, Cambridge, UK), followed by a secondary goat anti-mouse antibody (Abcam). The protocol was provided from the company. A DAB-peroxidase system (DAKO) was used for staining and hematoxilin for counterstaining.

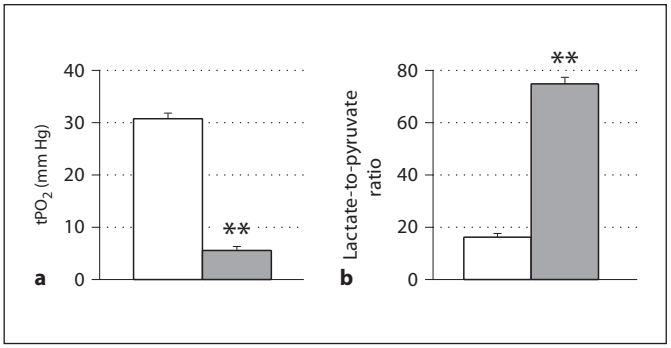

Fig. 2. a Partial tissue oxygen tension (mm Hg) and lactate-to-pyruvate ratio. The values of the flap tissue (black bar) are compared to measurements in control tissue (white bar). **b** The ptO_2 values correlate to the lactate-to-pyruvate ratio for normoxia in the control tissue and hypoxia in the flap tissue. Data are expressed as mean values and SD. ** $p < 0.01$ vs. control.

Positive and negative controls were taken for each antibody and between each step. Immunostaining was assessed qualitatively using light microscopy (Leica DM7RB, Wetzlar, Germany). Semiquantitative analysis was performed using a score system for staining intensity: 0 – no staining, 1 – fair staining, 2 – strong staining. Six samples per group were analyzed.

Statistical Analysis

The InStat version 3.0 software (Graph Pad Software, San Diego, Calif., USA) was used for statistical analysis. The data were presented as mean ± standard deviation (SD). Differences between groups were assessed by unpaired analysis of variance and Bonferroni correction. A value of $p < 0.05$ was taken to represent statistical significance.

Results

Hypoxia in the distal flap tissue was confirmed by a tpO_2 of 5.3 ± 0.9 versus 30.5 ± 1.2 mm Hg in controls ($p < 0.01$). Accordingly, the lactate-to-pyruvate ratio was 74.4 ± 8.5 in the distal flap compared to 15.7 ± 1.1 in controls ($p < 0.01$; fig. 2).

Analysis of microhemodynamic parameters revealed pathophysiological changes on different vascular levels. The conduit arterioles were enlarged in the critically perfused flap tissue over time (27.3 ± 4.4 and 29.4 ± 5.3 μm, respectively; $p < 0.01$ vs. control; fig. 3), whereas diameters remained at baseline in the control animals (20.3 ± 1.4 and 20.5 ± 2.8 μm on day 1 and 12). On the same vascular level, the tortuosity index was 1.35 ± 0.05 on day 12 versus 1.00 on day 1 ($p < 0.01$) in the flap tissue, while exhibiting no elongation in the control group. FCD was approximately 250 cm/cm^2 in the control tissue at

Downloaded from http://karger.com/esr/article-pdf/47/4/222/2738393/000333088.pdf by UniversitÄtsbibliothek Bern user on 21 June 2023

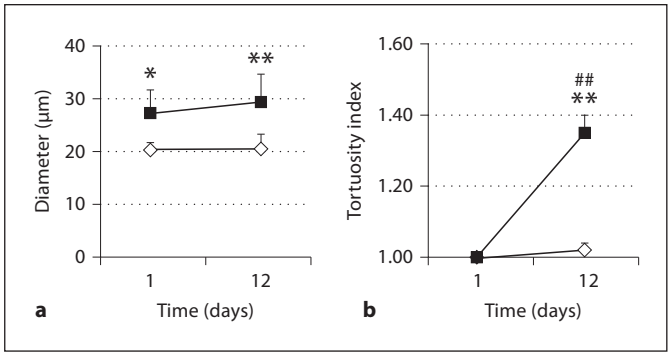

Fig. 3. Conduit collateral arterioles. **a** Change of diameter (μm) and **b** tortuosity index between day 1 and 12, measured by IVFM. Data are expressed as mean values and SD. Flap tissue: black symbols; controls: white symbols. * $p < 0.05$, ** $p < 0.01$ vs. control. ## $p < 0.01$ vs. day 1.

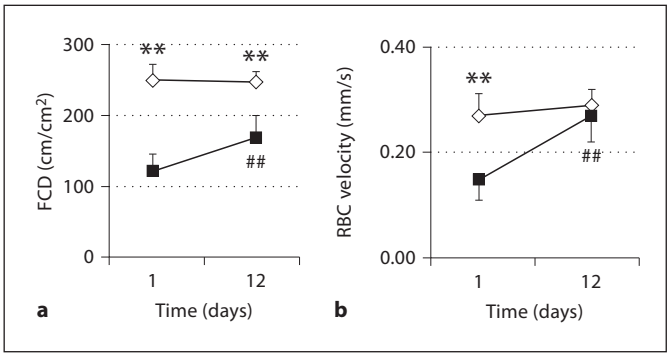

Fig. 4. Capillaries. **a** FCD (cm/cm^2) and **b** RBC velocity (mm/s). Data are expressed as mean values and SD. Flap tissue: black symbols; controls: white symbols. ** $p < 0.01$ vs. control; ## $p < 0.01$ vs. day 1.

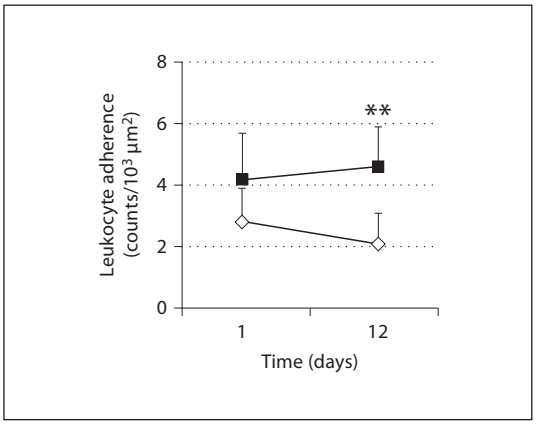

Fig. 5. Endothelial adherence of leukocytes: rollers and stickers (counts). Data are expressed as mean values and SD. Flap tissue: black symbols; controls: white symbols. ** $p < 0.01$ vs. control.

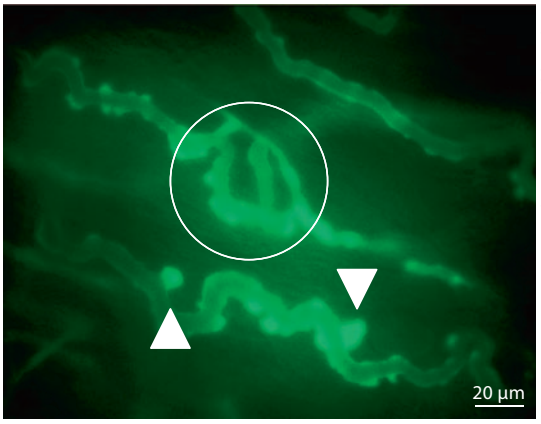

Fig. 6. IVFM of the flap in the dorsal skinfold chamber. Vascular morphology of capillaries showing tortuosity, buds, sprouts (arrowheads) and newly formed capillary structures (circle) as morphological equivalent of angiogenesis.

both time points. In the distal flap, FCD was reduced to 121.00 ± 25 cm/cm^2 on day 1, but recovered partially to 170 ± 30 cm/cm^2 on day 12 ($p < 0.01$ vs. day 1; $p < 0.01$ vs. control; fig. 4). Capillary RBC velocity on day 1 was 0.15 ± 0.04 mm/s in the distal flap tissue compared to 0.27 ± 0.04 mm/s in the control skin ($p < 0.01$), whereas values of 0.27 ± 0.05 and 0.29 ± 0.03 mm/s were obtained on day 12, respectively (fig. 4). The diameters in postcapillary collecting venules were similar in both groups and time points (data not shown). Increased counts of rolling and sticking leukocytes (4.2 ± 1.5 and 4.6 ± 1.3, respectively) were observed in the distal flap tissue at both days 1 and 12 (vs. 2.8 ± 1.1 on day 1 and 2.1 ± 1 on day 12; day 1 vs. day 12 n.s., day 12 control vs. flap $p < 0.01$; fig. 5).

Morphological evidence for angiogenesis and arteriogenesis could be demonstrated by IVFM in terms of sprouting and budding on capillary level (fig. 6) and increasing tortuosity on arteriolar level (fig. 7), respectively. The three-dimensional character of the remodeled microvasculature could be visualized with help of LSCM on capillary level (fig. 8).

Immunohistochemistry revealed strong positivity in the hypoxyprobe staining for hypoxic cells in the flap tissue (score 12/6) compared to controls (score 2/6) after 12 days. This was also true for the VEGF staining. Especial-

Color version available online

Downloaded from http://karger.com/esr/article-pdf/47/4/222/2738393/000333088.pdf by UniversitÄtsbibliothek Bern user on 21 June 2023

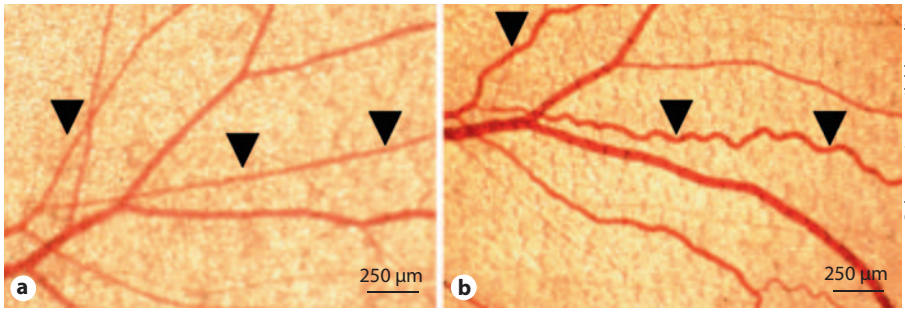

Color version available online

Fig. 7. Intravital light microscopy of the flap in the dorsal skinfold chamber. Corkscrew formation of collateral arteriole. Marked arterioles (arrowheads) on day 1 (**a**) and on day 12 (**b**) with increased elongation and tortuosity as morphological equivalent of vascular remodeling and arteriogenesis.

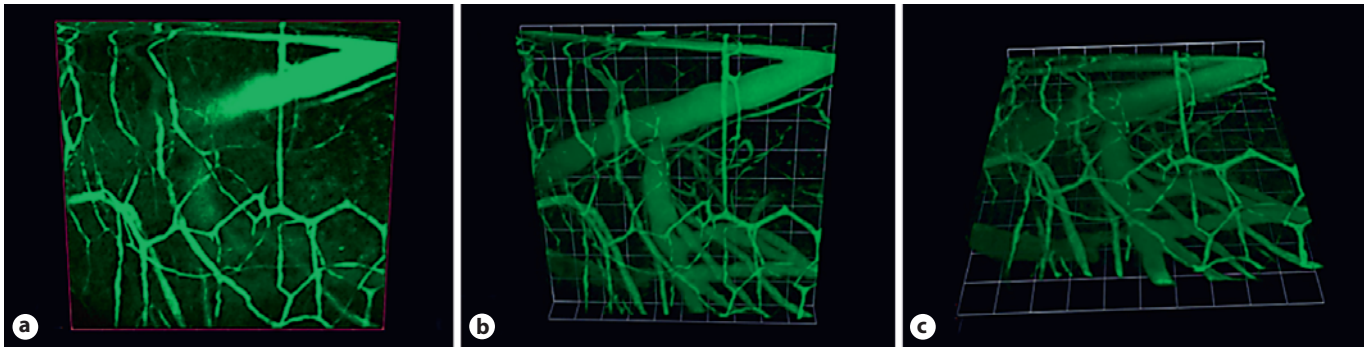

Color version available online

Fig. 8. Multiphoton LSCM. Single two-dimensional slide with capillaries and venules (**a**), and three-dimensional reconstruction of the same vascular area (**b**, **c**). Computer software enables virtual 360° animation for better imaging (one graphical unit = 50 μm).

ly the perivascular cells of arterioles and capillaries showed strong VEGF expression (score 10/6), whereas controls (score 3/6) did not show the same intensity of expression (fig. 9).

Discussion

In this new application of the dorsal skin fold chamber, we were able to demonstrate the functional and morphological results of vascular regeneration in an extended axial pattern flap with distal random perfusion. Physiological parameters as dilated and tortuous arterioles and increased capillary density and flow could be demonstrated. To our knowledge, this is the first in vivo documentation of combined arteriogenesis and angiogenesis in critical ischemia and the first three-dimensional reconstruction of angiogenesis in a surgical flap model. We could show in one model that vascular regeneration takes advantage of different mechanisms that contribute to hemodynamic improvements. Previous knowledge has shown that the survival of distant parts of axial pattern flaps is assured by vasodilation and recruitment of choke vessels, which is known as the delay phenomenon. In random pattern flaps, the survival was attributed to angiogenesis. Therefore, we provide a new view that a more complex system of vascular regenerating mechanisms is involved.

Various techniques have been used to investigate microcirculation and neovascularization in three-dimensional fashion, like corrosion casting [31], scanning electron microscopy [31, 32], microangiography [33, 34], but none has shown the technical promise of in vivo multiphoton LSCM so far [21, 22, 35]. Several advantages compared with other fluorescence-based microscopy techniques, including diminished phototoxicity, reduced bleaching, the phenomenon of second harmonic generation of ultraviolet photons by collagen fibers, which allows noninvasive imaging of extracellular matrix components and deeper tissue penetration (in our experience 250 μm for multiphoton excitation), have to be noticed. The two- and three-dimensional state-of-the-art fluorescence techniques allow for in vivo research utilizing fluorescent antibodies, nanoparticles and cells. The potential

Downloaded from http://karger.com/esr/article-pdf/47/4/222/2738393/000333088.pdf by UniversitÄtsbibliothek Bern user on 21 June 2023

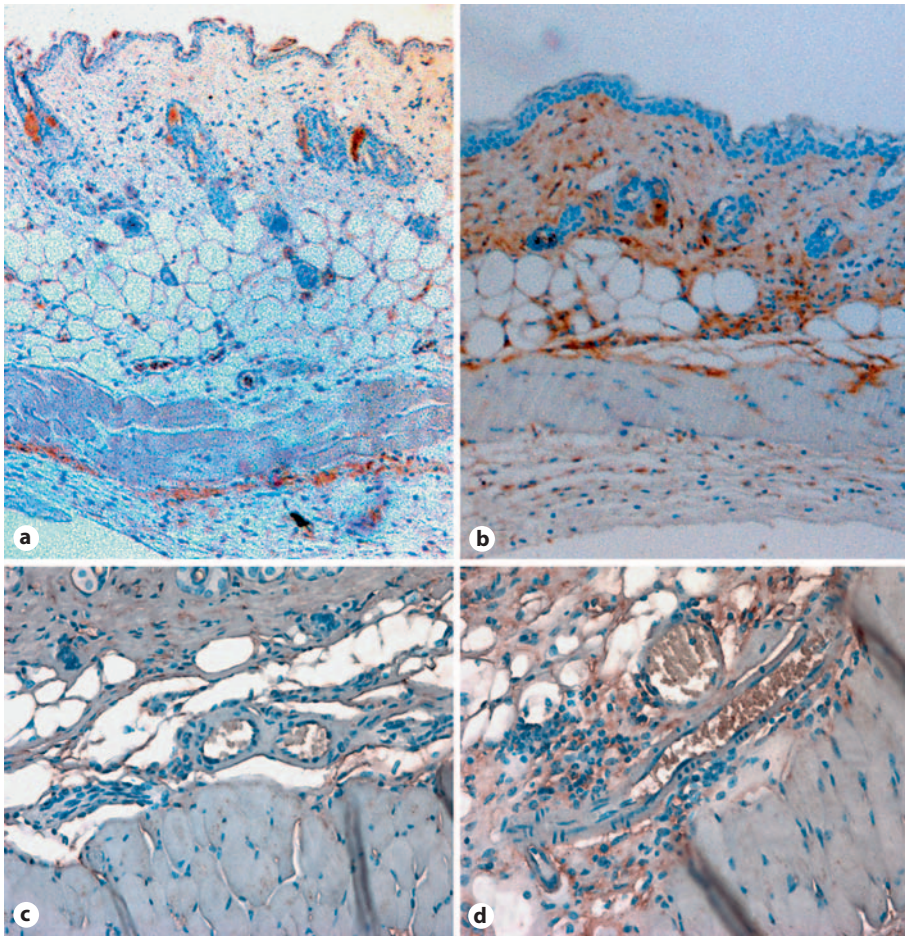

Fig. 9. Immunohistochemical sections. Hypoxyprobe staining of control skin fold chamber tissue (**a**) and flap tissue from the skin fold chamber (**b**). Auburn staining represents cells with positive hypoxia reaction. Differences of the morphology regarding the thickness of the subcutaneous adipose cell layer, the dermis and the size of the epidermal cell nuclei can be identified. VEGF staining in control skin fold chamber tissue (**c**) and flap tissue from the skin fold chamber (**d**). Flap vascularity is visualized with arterioles, venules and capillaries. Brown staining represents VEGF expression mainly in flap tissue (**d**).

implementation of fluorescent stem cells in our model is most promising for research of stem cell interaction in the context of vascular regeneration.

We standardized and characterized the flap tissue by quantitative and qualitative analysis of tissue oxygenation and oxygen metabolism utilizing microdialysis and partial tissue oxygen tension measurements in the same animals. Hypoxic tissue conditions due to critical ischemia could be demonstrated. Both methods have been used as standard procedures in our laboratory before [12, 27, 36]. Two approved models in experimental surgery were combined: (1) the dorsal skinfold chamber [6] and (2) a pedicled axially perfused skin flap at the dorsum of the mice [4, 5, 24]. This chronic model was evaluated for intravital microscopy investigation, without reaching a limit time-wise after 12 days. Quantitative measurements on microhemodynamic parameters in vivo without further need for invasive techniques or surgical manipulation were enabled. According to the literature, vascular regeneration has been studied mainly with a focus on one mechanism like arteriogenesis and angiogenesis [6, 8, 37]. This isolated point of view could be overcome with our new model through the combination of different microscopy techniques.

In detail, we found dilated and elongated conduit arterioles in the flap tissue, which equals the morphological result of arteriogenesis [38, 39]. The role of collateral vessels in this context has so far not been studied in extended flaps. The massive increase of tortuosity and vasodilation in collateral arterioles within the flap could be interpreted as shear stress-related vasodilation and trigger for elongation during arteriogenesis [39, 40]. Interestingly, the physiological and morphological changes had no influence on the capacity of the collecting venular system diameter, which could be due to constant outflow. Downstream to the arteriolar system, capillary budding and sprouting could be observed, resulting in angiogenetic recovery of FCD and RBC velocity. It remains speculative

Color version available online

Downloaded from http://karger.com/esr/article-pdf/47/4/222/2738393/000333088.pdf by UniversitÄtsbibliothek Bern user on 21 June 2023

if the recovery of capillary blood flow is mainly related to the partial recovery of FCD or the vasodilation on the arteriolar side. It could be assumed that both mechanisms contribute to it. Angiogenesis studied by IVFM has been described by Harder et al. [6] in a random pattern flap model in mice. However, this model was determined to focus on angiogenesis and demarcation against necrosis and not the integral process of vascular regeneration as in our model.

The increase of rolling and sticking leukocytes indicates a role of inflammatory response in vascular regeneration. Moreover, a defined role for adherent or activated leukocytes could be supposed [41]. As leukocytes can be effectively visualized in vivo, this could be of future interest for the use of our model.

In conclusion, this model could contribute to a better understanding of the different mechanisms of vascular regeneration by investigating the pathophysiological mechanisms of vascular remodeling on arterial, arteriolar, capillary and venular level in future experiments. Intense repetitive evaluation by intravital microscopy would result in monitoring of the morphological changes on different vascular levels and their hemodynamic relevance for the whole orchestrated process of vascular regeneration over time. The use of LSCM has so far not been described for in vivo chamber models in mice or flap models. In its complexity, it represents an ideal tool to investigate the effects of critical ischemia on arteriolar, capillary and venular morphology, microhemodynamic and vascular recovery processes separately for each vascular section. Inflammatory reactions on the level of leukocyte adhesion could be assessed and visualized, which opens the field of cellular research in vascular regeneration. Cell-cell interaction could be studied in addition as demonstrated by leukocyte adherence. Moreover, fluorescent intravital antibody staining and implementation of fluorescent stem cells would help to elucidate the contribution of resident and circulating progenitor cells to neovascularization, which is the direction of our future research projects.

Downloaded from http://karger.com/esr/article-pdf/47/4/222/2738393/000333088.pdf by UniversitÄtsbibliothek Bern user on 21 June 2023

References

1 Barker JH, Hammersen F, Bondar I, Galla TJ, Menger MD, Messmer K: Direct monitoring of nutritive blood flow in a failing skin flap: The hairless mouse ear skin-flap model. Plast Reconstr Surg 1989;84:303–313.

2 Erni D, Sakai H, Banic A, Tschopp HM, Intaglietta M: Quantitative assessment of microhemodynamics in ischemic skin flap tissue by intravital microscopy. Ann Plast Surg 1999;43:405–414; discussion 414–415.

3 Bertuglia S, Colantuoni A, Intaglietta M: Effect of leucocyte adhesion and microvascular permeability on capillary perfusion during ischemia-reperfusion injury in hamster cheek pouch. Int J Microvasc Clin Exp 1993; 13:13–26.

4 Ichioka S, Minh TC, Shibata M, Nakatsuka T, Sekiya N, Ando J, Harii K: In vivo model for visualizing flap microcirculation of ischemia-reperfusion. Microsurgery 2002;22: 304–310.

5 Tatlidede S, McCormack MC, Eberlin KR, Nguyen JT, Randolph MA, Austen WG, Jr: A novel murine island skin flap for ischemic preconditioning. J Surg Res 2009;154:112–117.

6 Harder Y, Amon M, Erni D, Menger MD: Evolution of ischemic tissue injury in a random pattern flap: A new mouse model using intravital microscopy. J Surg Res 2004;121: 197–205.

7 Spanholtz T, Maichle A, Niedworok C, Stoeckelhuber BM, Kruger S, Wedel T, Aach T, Middeler G, Hellwig-Burgel T, Bader A, Krengel S, Muller OJ, Franz WM, Lindenmaier W, Machens HG: Timing and targeting of cell-based VEGF165 gene expression in ischemic tissue. J Surg Res 2009;151:153–162.

8 Lindenblatt N, Calcagni M, Contaldo C, Menger MD, Giovanoli P, Vollmar B: A new model for studying the revascularization of skin grafts in vivo: The role of angiogenesis. Plast Reconstr Surg 2008;122:1669–1680.

9 Achauer BM, Black KS, Litke DK: Transcutaneous PO2 in flaps: A new method of survival prediction. Plast Reconstr Surg 1980; 65:738–745.

10 Potter RF, Peters G, Carson M, Forbes T, Ellis CG, Harris KA, DeRose G, Jamieson WG: Measurement of tissue viability using intravital microscopy and fluorescent nuclear dyes. J Surg Res 1995;59:521–526.

11 Contaldo C, Harder Y, Plock J, Banic A, Jakob SM, Erni D: The influence of local and systemic preconditioning on oxygenation, metabolism and survival in critically ischaemic skin flaps in pigs. J Plast Reconstr Aesthet Surg 2007;60:1182–1192.

12 Plock J, Frese S, Keogh A, Bisch-Knaden S, Ayuni E, Corazza N, Weikert C, Jakob S, Erni D, Dufour JF, Brunner T, Candinas D, Stroka D: Activation of non-ischemic, hypoxia-inducible signalling pathways up-regulate cytoprotective genes in the murine liver. J Hepatol 2007;47:538–545.

13 Popel A, Gross J: Analysis of oxygen diffusion from arteriolar networks. Am J Physiol 1979;237:H681–H689.

14 Groth L: Cutaneous microdialysis. Methodology and validation. Acta Derm Venereol Suppl (Stockh) 1996;197:1–61.

15 Harris A, Schropp A, Schütze E, Krombach F, Messmer K: Implementation of the microdialysis method in the hamster dorsal skinfold chamber. Res Exp Med 1999;199:141–152.

16 Rojdmark J, Blomqvist L, Malm M, Adams-Ray B, Ungerstedt U: Metabolism in myocutaneous flaps studied by microdialysis. Scand J Plast Reconstr Hand Surg 1998;32: 27–34.

17 Menger M, Sack F, Barker J, Feifel G, Messmer K: Quantitative analysis of microcirculatory disorders after prolonged ischemia in skeletal muscle. Res Exp Med 1988;188:151–165.

18 Menger MD, Barker JH, Messmer K: Capillary blood perfusion during postischemic reperfusion in striated muscle. Plast Reconstr Surg 1992;89:1104–1114.

19 Rucker M, Roesken F, Schafer T, Spitzer WJ, Vollmar B, Menger MD: In vivo analysis of the microcirculation of osteomyocutaneous flaps using fluorescence microscopy. Br J Plast Surg 1999;52:644–652.

20 Helmchen F, Denk W: Deep tissue two-photon microscopy. Nat Methods 2005;2:932–940.

21 Rubart M: Two-photon microscopy of cells and tissue. Circ Res 2004;95:1154–1166.
22 Brown EB, Campbell RB, Tsuzuki Y, Xu L, Carmeliet P, Fukumura D, Jain RK: In vivo measurement of gene expression, angiogenesis and physiological function in tumors using multiphoton laser scanning microscopy. Nat Med 2001;7:864–868.
23 Plock J, Contaldo C, Sakai H, Tsuchida E, Leunig M, Banic A, Menger M, Erni D: Is hemoglobin in hemoglobin vesicles infused for isovolemic hemodilution necessary to improve oxygenation in critically ischemic hamster skin? Am J Physiol 2005;289:H2624–H2631.
24 Vihanto MM, Plock J, Erni D, Frey BM, Frey FJ, Huynh-Do U: Hypoxia up-regulates expression of Eph receptors and ephrins in mouse skin. Faseb J 2005;19:1689–1691.
25 Contaldo C, Plock J, Djonov V, Leunig M, Banic A, Erni D: The influence of trauma and ischemia on carbohydrate metabolites monitored in hamster flap tissue. Anesth Analg 2005;100:817–822.
26 Schlosser S, Spanholtz T, Merz K, Dennler C, Banic A, Erni D, Plock JA: The choice of anesthesia influences oxidative energy metabolism and tissue survival in critically ischemic murine skin. J Surg Res 2009 [Epub ahead of print].
27 Schlosser S, Spanholtz T, Merz K, Dennler C, Banic A, Erni D, Plock JA: The choice of anesthesia influences oxidative energy metabolism and tissue survival in critically ischemic murine skin. J Surg Res 2010;162:308–313.
28 Contaldo C, Elsherbiny A, Lindenblatt N, Plock JA, Trentz O, Giovanoli P, Menger MD, Wanner GA: Erythropoietin enhances oxygenation in critically perfused tissue through modulation of nitric oxide synthase. Shock 2009;31:599–606.
29 Klyscz T, Junger M, Jung F, Zeintl H: [cap image – a new kind of computer-assisted video image analysis system for dynamic capillary microscopy]. Biomed Tech (Berl) 1997;42:168–175.
30 Zeintl H, Sack F, Intaglietta M, Messmer K: Computer assisted leukocyte adhesion measurement in intravital microscopy. Int J Microcirc Clin Exp 1989;8:293–302.
31 Lindenblatt N, Platz U, Althaus M, Hegland N, Schmidt CA, Contaldo C, Vollmar B, Giovanoli P, Calcagni M: Temporary angiogenic transformation of the skin graft vasculature after reperfusion. Plast Reconstr Surg 2010;126:61–70.
32 Rogers PA, Gannon BJ: The vascular and microvascular anatomy of the rat uterus during the oestrous cycle. Aust J Exp Biol Med Sci 1981;59:667–679.
33 Egana JT, Condurache A, Lohmeyer JA, Kremer M, Stockelhuber BM, Lavandero S, Machens HG: Ex vivo method to visualize and quantify vascular networks in native and tissue engineered skin. Langenbecks Arch Surg 2009;394:349–356.
34 Tirman WS, Caylor CE, Banker HW, Caylor TE: Microradiography; its application to the study of the vascular anatomy of certain organs of the rabbit. Radiology 1951;57:70–80.
35 Vajkoczy P, Farhadi M, Gaumann A, Heidenreich R, Erber R, Wunder A, Tonn JC, Menger MD, Breier G: Microtumor growth initiates angiogenic sprouting with simultaneous expression of VEGF, VEGF receptor-2, and angiopoietin-2. J Clin Invest 2002;109:777–785.
36 Plock JA, Rafatmehr N, Sinovcic D, Schnider J, Sakai H, Tsuchida E, Banic A, Erni D: Hemoglobin vesicles improve wound healing and tissue survival in critically ischemic skin in mice. Am J Physiol Heart Circ Physiol 2009;297:H905–H910.
37 Barker JH, Frank J, Bidiwala SB, Stengel CK, Carroll SM, Carroll CM, van Aalst V, Anderson GL: An animal model to study microcirculatory changes associated with vascular delay. Br J Plast Surg 1999;52:133–142.
38 Heil M, Schaper W: Influence of mechanical, cellular, and molecular factors on collateral artery growth (arteriogenesis). Circ Res 2004;95:449–458.
39 Schaper W, Scholz D: Factors regulating arteriogenesis. Arterioscler Thromb Vasc Biol 2003;23:1143–1151.
40 Carmeliet P: Mechanisms of angiogenesis and arteriogenesis. Nat Med 2000;6:389–395.
41 Carden DL, Smith JK, Korthuis RJ: Neutrophil-mediated microvascular dysfunction in postischemic canine skeletal muscle. Circ Res 1990;66:1436–1444.

Downloaded from http://karger.com/esr/article-pdf/47/4/222/2738393/000333088.pdf by UniversitÄtsbibliothek Bern user on 21 June 2023